CrossMark

RESEARCH PAPER

LC-MS/MS analysis of permethylated *N*-glycans facilitating isomeric characterization

Shiyue Zhou[1] · **Xue Dong**[1] · **Lucas Veillon**[1] · **Yifan Huang**[1] · **Yehia Mechref**[1]

Abstract The biosynthesis of glycans is a template-free process; hence compositionally identical glycans may contain highly heterogeneous structures. Meanwhile, the functions of glycans in biological processes are significantly influenced by the glycan structure. Structural elucidation of glycans is an essential component of glycobiology. Although NMR is considered the most powerful approach for structural glycan studies, it suffers from low sensitivity and requires highly purified glycans. Although mass spectrometry (MS)-based methods have been applied in numerous glycan structure studies, there are challenges in preserving glycan structure during ionization. Permethylation is an efficient derivatization method that improves glycan structural stability. In this report, permethylated glycans are isomerically separated; thus facilitating structural analysis of a mixture of glycans by LC-MS/MS. Separation by porous graphitic carbon liquid chromatography at high temperatures in conjunction with tandem mass spectrometry (PGC-LC-MS/MS) was utilized for unequivocal characterization of glycan isomers. Glycan fucosylation sites were confidently determined by eliminating fucose rearrangement and assignment of diagnostic ions, achieved by permethylation and PGC-LC at high temperatures, respectively. Assigning monosaccharide residues to specific glycan antennae was also achieved. Galactose linkages were also distinguished from each other by CID/HCD tandem MS. This was attainable because of the different bond energies associated with monosaccharide linkages.

Xue Dong, Lucas Veillon and Yifan Huang contributed equally to this work.

✉ Yehia Mechref
  yehia.mechref@ttu.edu

[1] Department of Chemistry and Biochemistry, Texas Tech University, Memorial Circle & Boston, Box 41061, Lubbock, TX 79409-1061, USA

Introduction

Glycosylation, one of the most common protein post-translational modifications (PTM), is essential in numerous biological processes [1–4]. However, comprehensive profiling of protein glycosylation is still a challenge despite the rapid development of bioanalytical techniques [5–7]. Several factors contribute to the complexity of glycosylation. The first is the size and uncertainty of added glycans. Unlike other PTMs such as phosphorylation, oxidation, and deamination, glycosylation usually introduces a large mass difference, thousands of Daltons, to the peptide backbone. The glycans often influence protein properties and adversely influence the tandem MS analysis of glycopeptides. Therefore, sequencing is generally not as effective as MS-based peptide mapping. The second factor is the complexity of glycosylation. Although the monosaccharides (seven basic types, *N*-acetylglucosamine, *N*-acetyl galactosamine, galactose, mannose, fucose, *N*-acetylneuraminic acid, and *N*-glycolylneuraminic acid) involved in the biosynthesis of glycans is limited, possible branching of glycans significantly increases the number of possible structures synthesized with the same composition but with different branching [8]. Moreover, there are multiple types of

linkages for connecting monosaccharides to each other [9, 10], resulting in numerous isomeric glycan structures [11]. The third factor that makes glycomic analysis challenging is the labile features of glycans. The glycosidic bond of a glycan is weaker than peptide bonds. Hence, monosaccharide losses during MS analysis are common. Sialic acid loss [12] or fucose migration and rearrangement [13, 14] in the gas phase during matrix-assisted laser desorption ionization (MALDI) or electrospray ionization (ESI) and MS/MS analysis are a direct result of weak glycosidic bonds.

Efforts to define protein glycosylation using tandem mass spectrometry have been ongoing since the late 1980s [15]. Among the fragmentation techniques available, collision-induced dissociation (CID) has proven to be widely applicable for the generation of tandem mass spectra of oligosaccharides [16]. The technique is characterized by the acceleration of analyte molecules and their subsequent collision with a neutral gas which results in the fragmentation of molecular bonds and the creation of tandem mass spectra [17]. Following the development of the Orbitrap MS, Olsen and coworkers [18] introduced a CID-related fragmentation technique, termed higher-energy collisional dissociation (HCD), where beam-type fragmentation spectra were created inside the C-trap. This higher energy technique does not suffer from the so-called 1/3 rule that dictates the lower range m/z cutoff that limits ion-trap CID and therefore may be utilized for the detection of individual monosaccharide fragments. In this study, CID and HCD are combined to characterize the composition and linkage of permethylated N-glycans.

Although the directed analysis of glycoproteins provides more site-specific information of glycans, structural elucidation is difficult due to the influence of the peptide backbone. Analyzing released glycans is a more realistic strategy for comprehensive glycomic profiling of glycoproteins. Glycans lack chromophore or fluorophore moieties to enable optical detection and exhibit low ionization efficiencies in MS analysis. Hence, derivatization is always utilized in glycomic profiling studies. There are several limitations associated with spectroscopy-based glycomic analysis because the identification of glycans in this strategy relies on retention time during separations such as liquid chromatography (LC) [19–21] and capillary electrophoresis (CE) [22, 23]. In this case, only known glycan structures can be identified by the platforms. Meanwhile, baseline resolution is required for all glycans in the sample during the separation; this is possible for the analysis of a small number of glycoproteins, but challenging in the analysis of glycans derived from complex biological samples such as whole blood, cell lines, and tissues. MS, as one of the most powerful bioanalytical instruments, brings glycomic analysis one step further because of its capability of compositionally identifying glycans. Although high-resolution MS or triple quadrupole MS provides accurate identification of glycan sequences, more work is needed to comprehensively elucidate glycan structures through tandem MS.

The initial criteria for glycan structure analysis through tandem MS is the efficient separation of different isomers [19, 24–51]. Hydrophilic interaction liquid chromatography (HILIC-LC) is the most efficient separation method for native or reducing end-labeled glycans that provides efficient separation of different isomers [19, 21, 45]. Several databases have been established to facilitate characterization of glycans by HILIC-LC [52, 53]. The combination of HILIC-LC with tandem MS has enabled the identification of many glycan isomers [54]. However, sialic acid loss and fucose migration and rearrangement often generate misleading fragments and hinder structural assignment [13, 55].

Permethylation is a common derivatization method that is usually employed to stabilize glycan structures and improve ionization efficiency [56, 57]. The influence of labile glycan structures in tandem MS is mitigated by permethylation. Moreover, permethylation also improves the fragmentation pattern of glycans in MS/MS analysis, and more fragments resulting from glycosidic bond breakage can be generated [57–64]. However, the isomeric separation of permethylated glycans using existing methods is not satisfactory. This problem prevented the permethylation strategy from becoming the most effective glycan structure analysis method because isomeric separation is presently considered a basic criterion for the comprehensive characterization of glycans.

In our recent study, we demonstrated that the application of elevated temperatures resulted in the partial isomeric separation of permethylated glycans on C18 [27]. Isomeric separation of permethylated glycans using PGC-LC-MS/MS at room temperature was first reported by Costello and co-workers [65]. Here, we employ a strategy that builds upon previous studies where porous graphitic carbon (PGC) was applied for the separation of native alditols [66–71] in addition to our own work where an optimized high-temperature PGC-LC method was implemented for the isomeric separation of permethylated glycans in human and bovine milk samples [26, 72]. Both monosaccharide site isomers and linkage isomers can be baseline resolved in this strategy. With the help of an established separation technique for permethylated glycans coupled with optimized CID and an HCD MS/MS method, we are able to distinguish between glycan isomers by tandem MS. The described approach enabled the identification of fucose and galactose site isomers, as well as galactose linkage isomers, and expands upon our previous studies [26, 27, 72] by extending the diversity of isomeric structures characterized by tandem MS to include complex glycans from model glycoproteins as well as human serum.

Materials and methods

Materials

Fetuin, ribonuclease B, and pooled human blood serum were purchased from Sigma-Aldrich (St. Louis, MO). IgG standard was provided from Waters (Milford, MA). HPLC-grade acetonitrile, water, formic acid, methanol, and isopropanol were bought from Fisher Scientific (Pittsburgh, PA). Sodium hydroxide beads and ammonium borane complex were purchased from Sigma-Aldrich (St. Louis, MO). PNGase F and corresponding digestion buffer were obtained from New England Biolab (Ipswich, MA).

Glycan release, reduction, and permethylation

Glycoproteins or blood serum samples were first mixed with PBS buffer (20 mM, pH 7.5) and thermally denatured in a 90 °C water bath for 20 min. After the denatured sample was cooled to ambient temperature, approximately 100 U of PNGase F was added to each sample and incubation was conducted in a 37 °C water bath for 18 h [73]. After PNGase F digestion, protein was removed by precipitation using 90 % ethanol. The purified glycans were then subjected to reduction using a procedure based on a method for the reductive β-elimination of *O*-linked oligosaccharides [74]. An aqueous 10 μg/μL ammonium borane complex solution was prepared. Ten microliters of ammonium borane solution was added to each sample and incubated in a 60 °C water bath for 1 h. After incubation, 400 μL of methanol was added to each sample which was then dried using a centrifugal vacuum concentrator. This step was repeated three to four times until excess ammonium borane was removed. The dried reduced sample was resuspended in 1.2 μL of water, 30 μL DMSO, and 20 μL of iodomethane for permethylation. A solid-phase permethylation protocol was utilized in this study [57]. A spin column was packed by transferring DMSO-soaked sodium hydroxide beads using a micropipette; then DMSO was forced out by centrifugation. The sample mixture was then applied to the prepared reaction spin column. After 25 min of incubation, 20 μL of iodomethane was added to the spin column. After another 15 min of incubation, the permethylated glycans were eluted using 100 μL of acetonitrile. The eluent was then dried using a centrifugal vacuum concentrator because of the existence of DMSO and a high concentration of salts. Finally, the dried sample was resuspended in a 20 % acetonitrile, 0.1 % formic acid solution for LC-MS/MS analysis.

LC-MS methods

The separation was conducted using an UltiMate 3000 nano UHPLC system, and the column for separation was a HyperCarb PGC column (75 μM × 150 mm, 5 μM particle size; Thermo Scientific, Pittsburgh, PA). The oven temperature was set to 75 °C, an optimized value reported in a previous publication of ours [27]. Mobile phase A was composed of water and 0.1 % formic acid, and mobile phase B consisted of 98 % acetonitrile, 2 % water, and 0.1 % formic acid. In the first 10 min, online purification was conducted using a trap to remove the salts generated during permethylation. The flow rate for LC separation was 0.65 μL/min. Then the analysis gradient started at 40 % of mobile phase B. The percentage of B increased to 75 % in 15 min and subsequently increased to 95 % in 20 min. The 95 % mobile phase B was kept for 15 min and brought back to 20 % to reestablish equilibrium. The LC was connected to an LTQ Orbitrap Velos mass spectrometer (Thermo Scientific, San Jose, CA) by nanoESI, which was operated using a 1.6-kV ESI spray voltage. Three events were set in each scan cycle. The first event was a full MS scan acquired at 60,000 resolution with a *m/z* range of 500 to 2000. The second and third events were data-dependent MS/MS scans following the first event. The top four most intense ions were subjected to CID and HCD MS/MS. Dynamic exclusion was enabled to exclude ions repeated within 20 s. The energy used for HCD was 45 % normalized collision energy, optimized, in previous studies [75–77] while 30 % normalized collision energy was used for CID, which was also previously optimized [78]. A mass tolerance of 10 ppm was used for extracted ion chromatograms (EICs) of full MS data. The mass accuracy for CID fragmentation in the ion trap (IT) was within the range of *m/z* ±0.5.

Data interpretation

Glycan compositions were first identified using EIC of full MS data with a 10-ppm mass tolerance. After determining the retention time for each glycan isomer, the MS/MS scans that were acquired during the retention time ranges of interest were analyzed for structure elucidation. GlycoWorkbench was utilized to generate the mass list of all possible glycan fragments. Manual assignment was performed to match the peaks in the MS/MS spectra with the theoretical fragment mass list.

Results and discussion

To achieve an unequivocal structural characterization of *N*-glycans, it is necessary to determine the carbohydrate composition, sequence, and branching of monosaccharides, interglycosidic linkages, and anomeric connectivity. Although it is often analytically challenging, it is also necessary to explicitly define the occupancy of oligosaccharide antennae, galactose linkages, and the location of fucosylation sites. Several analytical techniques have been developed to address such needs; however, each has its pros and cons [35, 40, 44, 79–98].

Chemical reduction of glycans-free reducing ends is necessary to eliminate glycan anomers, which complicate LC analysis. Moreover, chemical reduction imparts a mass difference to the reducing end GlcNAc, thus facilitating its distinction from other internal GlcNAc moieties. Chemical reduction of the reducing end of a glycan can be considered as labeling with two hydrogens from the perspective of molecular weight. Permethylation not only stabilizes glycan structures and enhances MS signals but also simplifies tandem MS interpretation. Tandem MS of permethylated glycans provides information regarding the location and sequence of monosaccharides in a structure [57–64]. Two examples are listed in Table 1. The first pair of glycan fragments, consisting of a galactose and GlcNAc residue, provides an example illustrating that it is possible to identify whether there is a branching monosaccharide connected to a glycan ring. When there is one monosaccharide that has been attached that is lost during MS/MS analysis, the previous attachment site will be converted to a hydroxyl group (see Table 1 illustration associated with m/z 450.23). In the case

that the site was not occupied, the hydroxyl group would have been exposed to permethylation and converted to a methoxy group. Hence, a 14-Da mass difference will be created, and the occupancy of glycan branching is revealed. In comparison, for native or reducing end-labeled glycans, such a difference does not exist because there is no methyl group modification during derivatization. Reducing and permethylation permit the identification of the reducing end GlcNAc. When a glycan is reduced and permethylated, a reducing end GlcNAc with fucose has a m/z value of 468.27 while a non-reducing end GlcNAc with fucose has a m/z value of 438.24 (Table 1). The mass difference is generated by the addition of two hydrogens and two additional permethylation sites, which add 28 Da to the reducing end. However, for the non-reduced native glycan, these two fragments are identical in mass (Table 1).

In addition to the abovementioned limited tandem MS information associated with native and reducing end glycans, fucose migration is common and results in misleading fragment ions. Figure 1a is the MS/MS spectra of a native glycan

Table 1 Examples of mass differences for glycan fragment ions resulting from tandem MS of native or chemically reduced and permethylated glycans


The m/z of all the fragments reported are singly protonated ions. Purple circles indicate the sites of cleavages. Red labels indicate the atoms and functional groups prompting differences in m/z values between native and permethylated glycans

standard whose structure is already determined. This is a branch fucosylated glycan, and most of the fragments in the MS/MS spectra can be assigned to its correct structure. However, the fragments at *m/z* values of 897.43 and 1059.43 are representing the glycan core structure with the addition of a fucose moiety. These fragments indicate that there is a small number of fucose residues that migrated from a branch to the glycan core. Figure 1b is the MS/MS spectra of a RapiFluor-MS labeled IgG glycan, in which the fucose is expected to be a core fucose. Although most fragments agree with this structure, there is one fragment at *m/z* 512.27 that can be assigned to fucose on the same branch as galactose. This is evidence of fucose migrating from the glycan core structure to a branch. Both examples demonstrate the migration of fucose in the gas phase for native and reducing end-labeled glycans. As shown below, such migration could be overcome by permethylation which eliminates all active sites possible for fucose migration.

As aforementioned, the fragment of reducing end GlcNAc plus a fucose at *m/z* 468.27 could be utilized as a diagnostic ion for the identification of core fucosylation. It is essential to elucidate the fucosylation site in a glycomic analysis because of the biological attributes of fucose on different sites. MS/MS spectra of a core fucosylated glycan exhibited a fragment ion with a *m/z* 468.27 ion, while no such ion is observed in the MS/MS spectra of a branch fucosylated structure. Figure 2a is the parent ion scan of the diagnostic core fucosylation fragment ion at *m/z* 468.27 in all MS/MS spectra in an LC-MS/MS analysis of glycans released from human blood serum. The

Fig. 1 CID MS/MS spectrum for (**a**) reduced native glycan standard with branch fucosylation and (**b**) RapiFluor-MS labeled IgG glycan. The mass shift generated by the RapiFluor-MS tag from native glycans with a free reducing end is equal to 311.3815 Da. All fragment ions reported in both panels (**a**) and (**b**) are singly charged protonated species, excepting *m/z* 867.7 in panel (**b**), which is doubly protonated
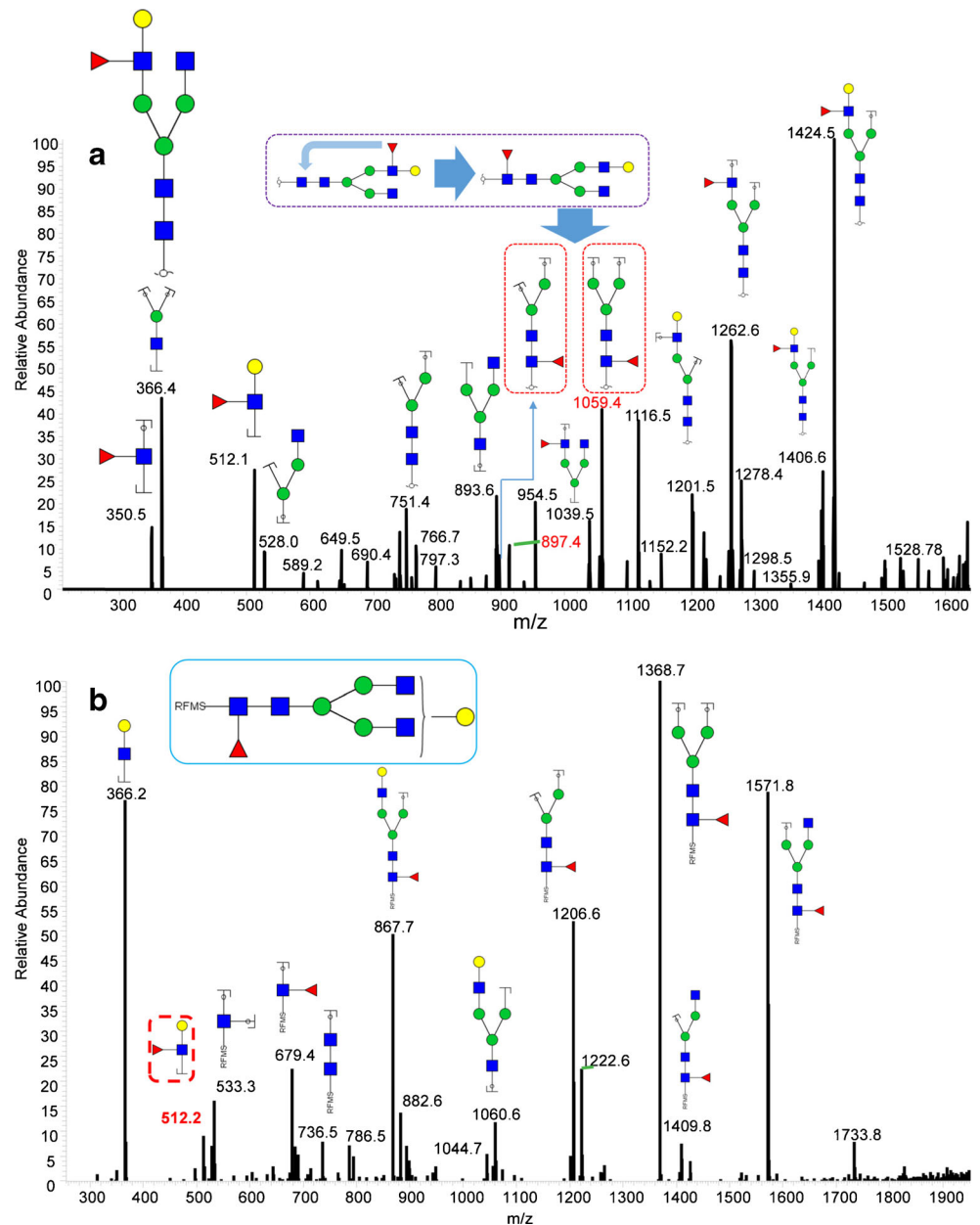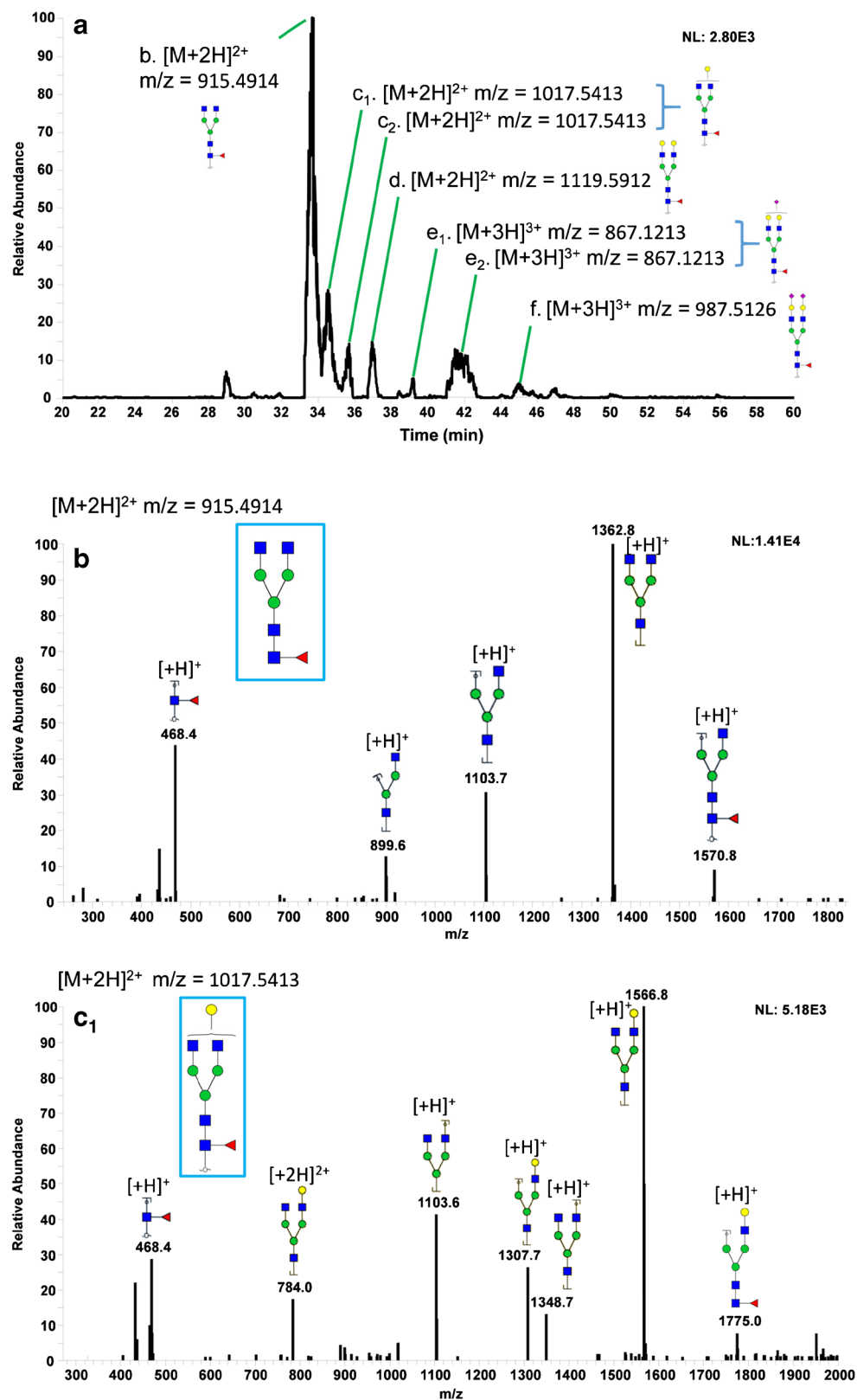
Fig. 2 Precursor ion scan of a diagnostic ion to detect core fucosylation of reduced and permethylated *N*-glycans derived from human blood serum (**a**). CID MS/MS spectra for F1A2 (**b**), F1A2G1 (**c₁** and **c₂**), F1A2G2 (**d**), F1A2G2S1 (**e₁** and **e₂**), and F1A2G2S2 (**f**). Figure labels match peak labeling

first peak overlapped with the full MS EIC of an F1A2 glycan, which is mainly from IgG in human blood and is already known as a core fucosylated glycan. The MS/MS fragmentation spectra of *m/z* 915.4914, shown in Fig. 2b, support the
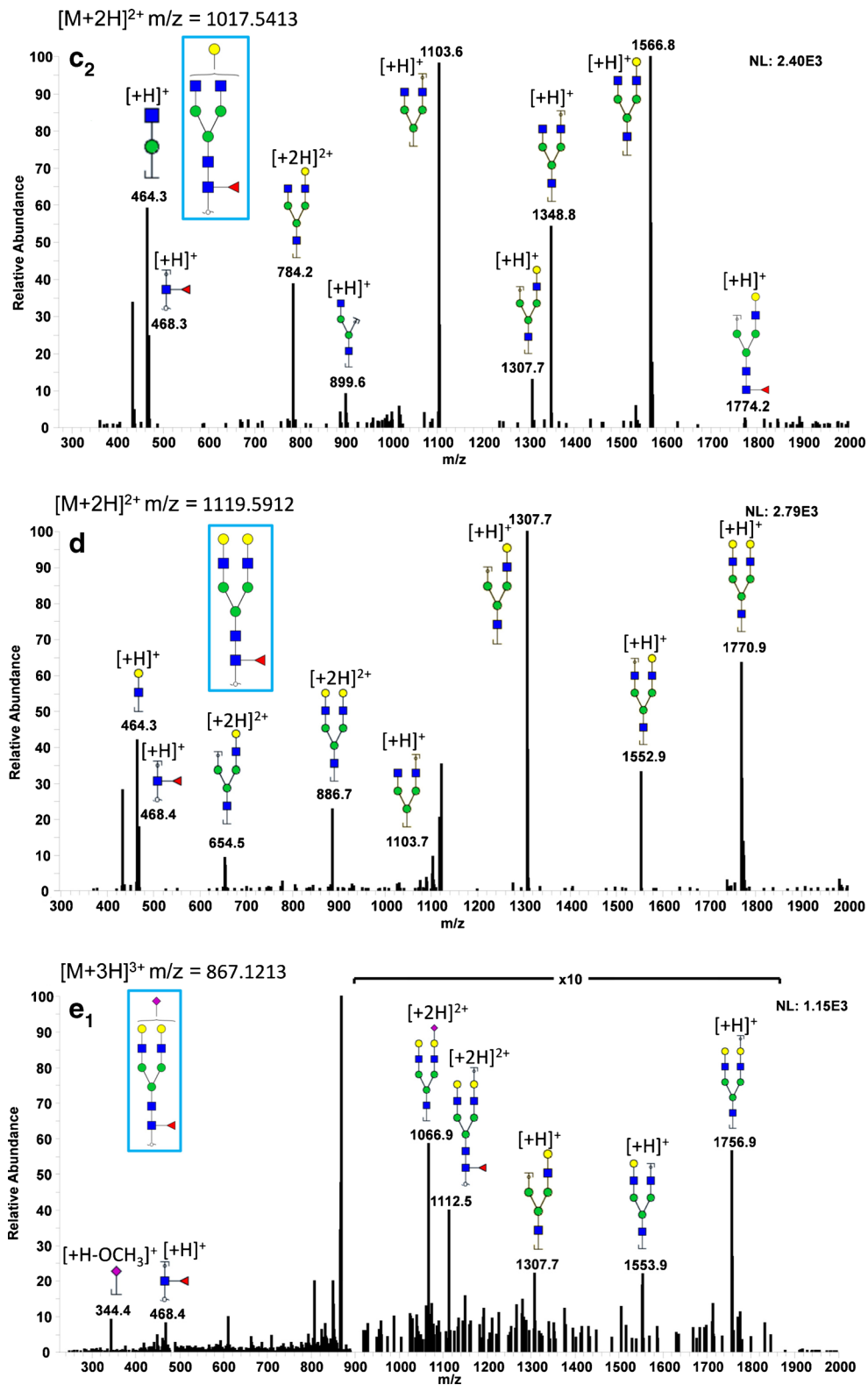
Fig. 2 (continued)

identification of this first peak as F1A2 demonstrating fragments corresponding to the intact structure minus a single branched GlcNAc and the fucosylated core GlcNAc residue at m/z 1570.8 and 1362.8, respectively. The second and third peaks can be matched to F1A2G1 structures, which are also mainly from IgG in human blood serum and demonstrated as core fucosylated. These two separated peaks result from the isomeric separation of galactose on different branches, further
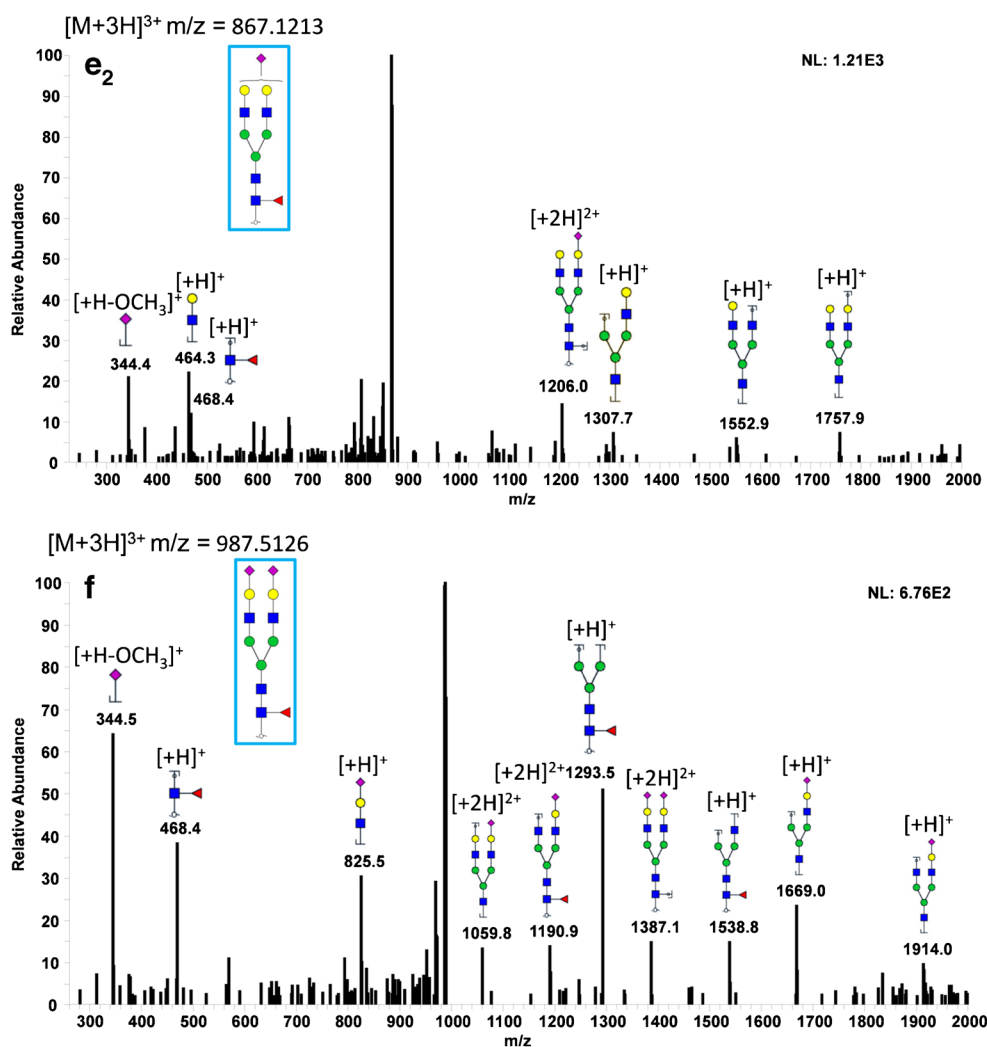
Fig. 2 (continued)

demonstrating the isomeric separation capability of PGC-LC for permethylated glycans.

Two MS/MS spectra of *m/z* 1017.5413 are shown in Fig. 2c₁ and c₂, corresponding to the two peaks labeled as c₁ and c₂ in Fig. 2a, respectively. The two spectra have near identical diagnostic fragments that differ only in their relative ratios, an observation typical of structural isomers. Despite similar fragmentation spectra, these isomers can be differentiated based on retention time with peak c₁ (Fig. 2a and c₁) corresponding to the isomer, with a retention time of 34.56 (Fig. 3a), with galactose attached to the Man α1–6 arm and peak c₂ (Fig. 2a and c₂) being identified as the structure, with a retention time of 35.64 (Fig. 3a), with galactose attached to the Man α1–3 arm. Similarly, the core fucosylation diagnostic ion for F1A2G2 can also be observed in MS/MS spectra of *m/z* 1119.5912 displayed in Fig. 2d. Several sialylated and core fucosylated structures were also noted (Fig. 2a, e₁, e₂, and f), and the separation of different sialic acid linkages were seen (Figs. 2a, e₁, e₂, and 3b). Using the elution order detected, we

were able to designate peaks e₁ and e₂ as F1A2G2S1 with an α2–3 and α2–6 linked *N*-acetylneuraminic acid (Figs. 2a, e₁, e₂, and 3b), respectively. The EIC of F1A2G2S1, at *m/z* 867.1213, illustrates the separation of two isomers in addition to the most abundant α2–3 and α2–6 linked structures identified with retention times of 38.43 and 38.43 min, respectively (Fig. 3b). Due to the weak intensity of these low abundance isomers, a sufficient number of MS/MS scans were not collected for their definitive characterization. Taken together, we can confidently conclude that the fragment of reducing end GlcNAc plus a fucose at *m/z* 468.27 can be used as a diagnostic ion for identifying core fucosylation. However, it should be mentioned that *N*-glycan structures containing α1–3 linked core fucose were not examined in this study due their resistance to PNGase F cleavage [99].

We also utilized the above-described combination of PGC-LC and tandem MS of permethylated glycans to identify isomers resulting from different galactose linkages. Galactose can be linked to GlcNAc by either β 1,3 or β 1,4 linkage.

Fig. 3 Extracted ion chromatogram (EIC) for two reduced and permethylated F1A2G1 isomeric structures, $[M + 2H]^{2+}$, at *m/z* 1017.5413 (**a**) and four reduced and permethylated F1A2G2S1 isomeric structures, $[M + 3H]^{3+}$, at *m/z* 867.1213 (**b**)
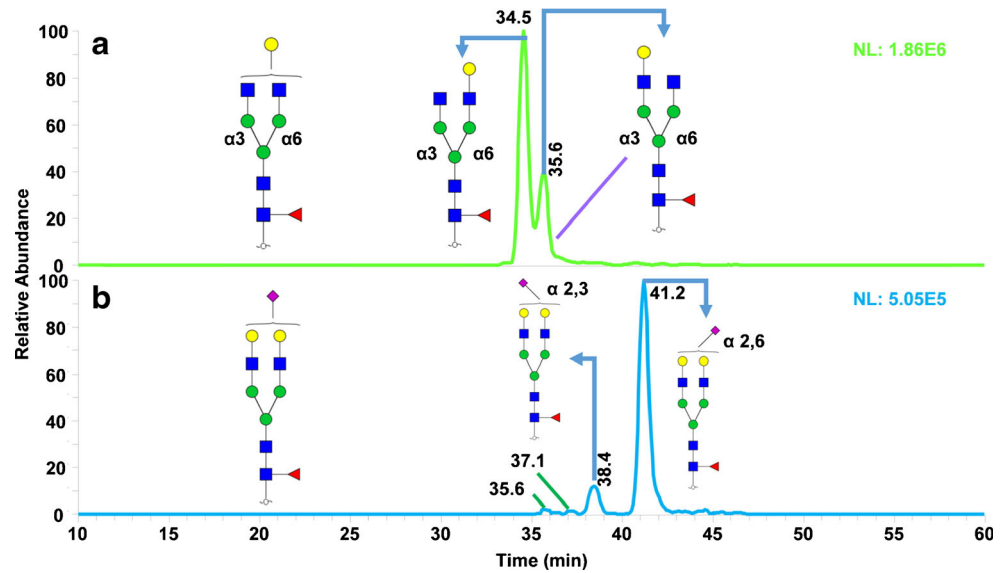
Here, we selected glycans released from fetuin for our study because the structures of fetuin glycans are already fully elucidated by previous NMR studies [100–102]. Both β 1,3 and β 1,4 linkages exist in the tri-antennary structure of fetuin according to the NMR data. In order to eliminate the influence of different sialic acid linkages, we conducted sialidase treatment prior to analysis to remove all sialic acids from fetuin glycans. Figure 4a is the EIC for glycan A3G3; there were two isomeric peaks observed at 38.3 and 48.2 min. According to the intensity ratio from the NMR data [101], we can assign the first peak to be the one where all galactoses are β 1,4 linked, and the later peak corresponds to the glycan that has the middle galactose β 1,3 linked. In order to confirm that this assignment is correct, we conducted a linkage-specific glycosidase array to check the galactose linkages. First, the sample was

treated with β 1,3 galactosidase [103, 104], which only removes β 1,3 linked galactose. After the treatment, the first peak at 38.3 min remains intact with the same *m/z* value and retention time as shown in Fig. 4b, indicating that the first isomer has no β 1,3 linked galactose. The second peak at 48.2 min disappeared, and the peak of A3G2 appeared at 32.5 min (Fig. 4c). These results indicated that the second peak is a glycan with one β 1,3 linked galactose. β 1,4 galactosidase was also utilized to treat the sample [103]. Following treatment, the peak at 38.3 min disappeared, and the peak of A3 appeared at 26.4 min (Fig. 4d) because all galactose residues were cleaved from the first isomer, while the second isomer was converted to A3G1 at 30.3 min (Fig. 4e), indicating that the second isomer has one galactose connected with β 1,4 linkage. Moreover, the intensity ratio of the two isomers


Fig. 4 EIC for reduced and permethylated fetuin tri-antennary glycans after treatment with sialidase (**a**), β 1,3-galactosidase (**b, c**), and β 1,4-galactosidase (**d, e**)
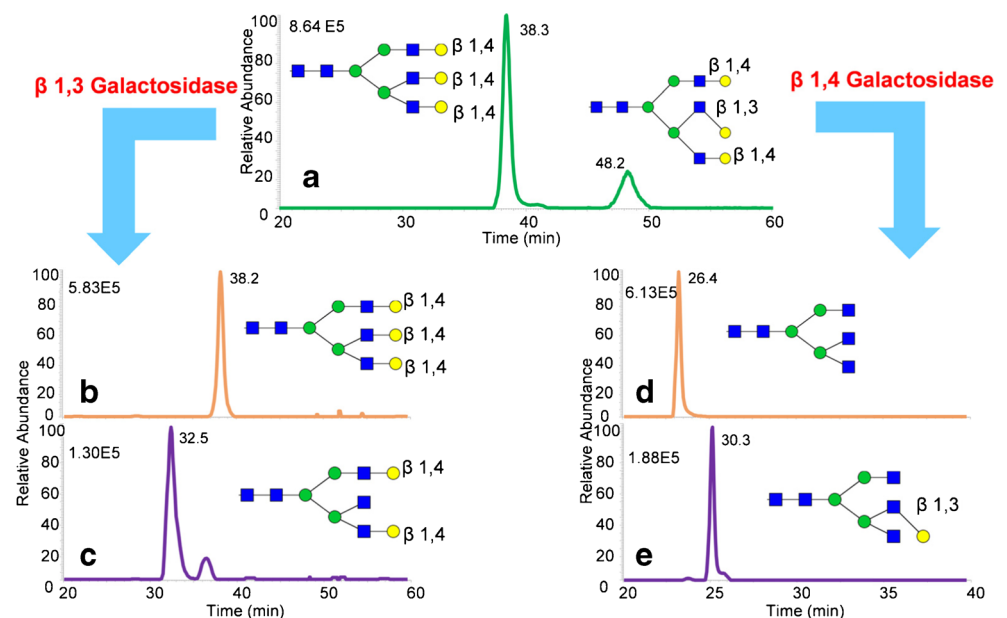
remained consistent before and after galactosidase treatment. All these observations support the validity of the isomer assignment. However, the purpose of this study is to elucidate glycan structure without the help of a glycosidase array, with our goal being to collect all required information from a single LC-MS/MS run.

We next evaluated the CID MS/MS spectrum for both structures. In order to acquire MS/MS spectra of sodiated ions at high ion yields and high quality, glycans released from fetuin were resuspended in a 0.2 M sodium chloride solution to prompt the formation of precursor ions of sodiated adducts [105]. As shown in Fig. 5a, both structures resulted in similar

Fig. 5 CID MS/MS spectra (**a**, **b**) and HCD MS/MS spectra (**c**, **d**) for two reduced and permethylated fetuin tri-antennary glycan isomers, [M + 2H]$^{2+}$, that only differ in the linkage of one terminal galactose residue
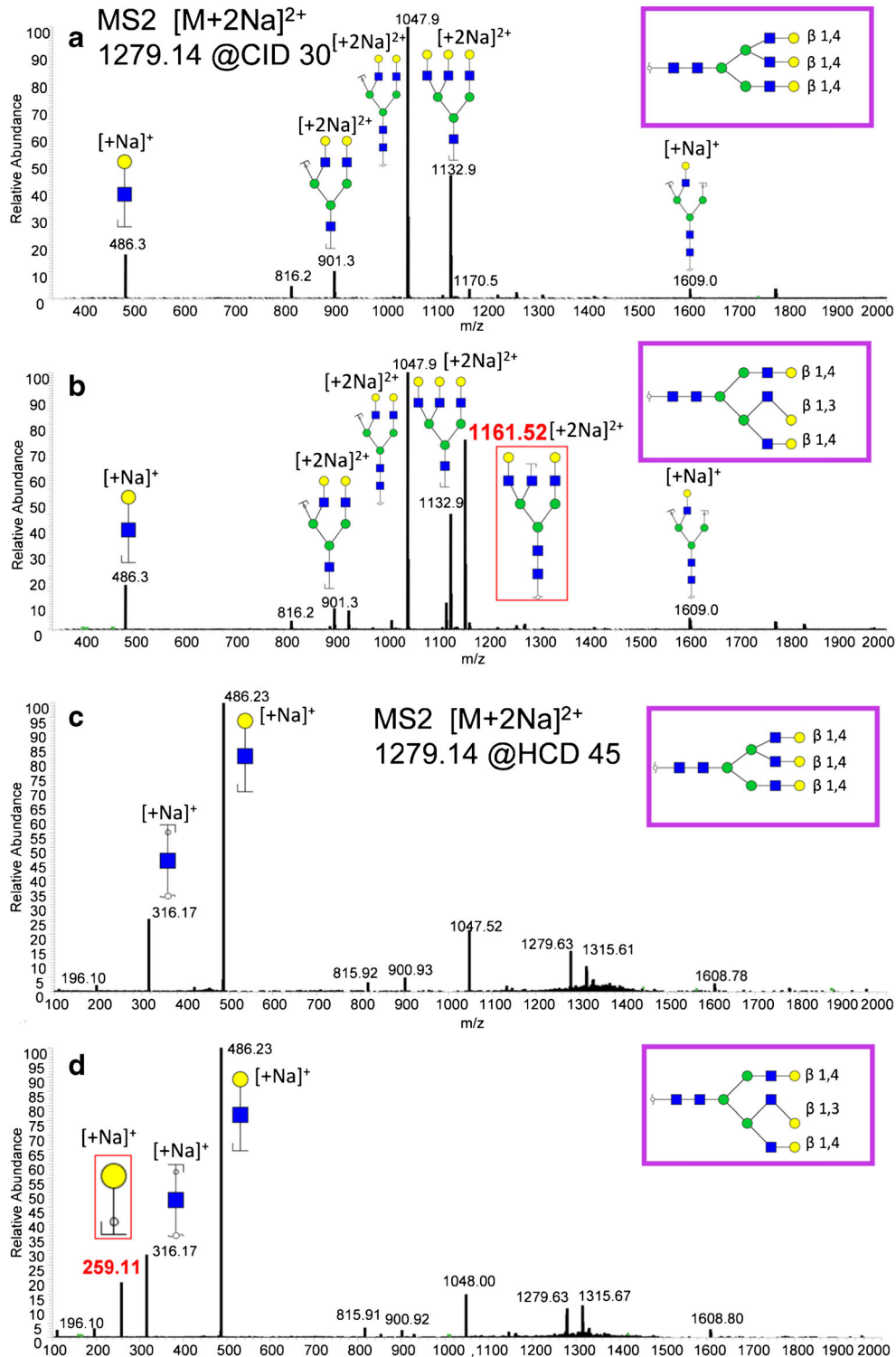
fragments with similar intensity. However, there is one significant peak at *m/z* 1161.52 in the lower trace. This fragment can be assigned to a doubly charged fragment that results from losing one galactose from the precursor ion. This MS/MS spectrum demonstrated that the later eluting isomer contains one unique galactose that is different from the other galactoses. This observation agreed with our expectation of the isomer structure. Since we can see the unique peak at *m/z* 1161.52 for the β 1,3 linked galactose, we should also observe the fragment of the released galactose. However, this was not seen in the CID MS/MS spectrum due to the limitations of an ion trap instrument; the cutoff of detection is one third of the *m/z* value of the precursor ion. In this case, ions smaller than *m/z* 400 could not be seen in CID.

The advantage of using a CID/HCD double-play MS/MS method is reflected in this case. HCD provides different fragmentation patterns and has no one-third cutoff detection limit. In the HCD spectrum in Fig. 5b, most fragments are identical except for the unique fragment at *m/z* 259.11 in the MS/MS spectra for the later eluting isomer. The fragment at *m/z* 259.11 can be assigned to a free galactose, and this finding perfectly matched our expectation based on the CID MS/MS data. Hence, we can draw the conclusion that the bond energies of β 1,3 and β 1,4 linked galactoses are different, prompting different fragmentation patterns in both CID and HCD MS/MS. The bond energy of the β 1,3 linkage is greater than the bond between mannose and GlcNAc. Therefore, GlcNAc plus galactose fragments can only be found during MS/MS analysis if all galactose residues are β 1,3 linked. Free galactose fragments or precursor ions minus one galactose will be found when there exists β 1,4 linked galactose because the bond energy of the β 1,4 linkage is weaker than the bond between mannose and GlcNAc. This analysis demonstrates the necessity of employing orthogonal MS/MS methods during analysis to cover different *m/z* ranges and provide more structural information.

Conclusion

In this study, we utilized the capability of PGC-LC in separating permethylated glycans to conduct glycan isomeric structure elucidation by tandem MS. Isomers from variable fucosylation sites and galactose linkages were successfully separated using LC and identified by CID and HCD MS/MS. Fucose migration in the gas phase was overcome by permethylation. In agreement with our previous study [26], involving milk oligosaccharides, we report a diagnostic ion at *m/z* 468.27 that can be utilized for the identification of core fucosylation. Tandem MS was also employed to distinguish galactose residues attached to the 3- or 6-antenna of a biantennary glycan structure. β 1,3 and β 1,4 linked galactose residues have different bond energies that prompted the yield

of unique fragments that facilitated the identification of glycan structures.

Compliance with ethical standards

Conflict of interest The authors declare no competing financial interest and no conflict of non-financial interests.

References

1. Varki A. Glycan-based interactions involving vertebrate sialic-acid-recognizing proteins. Nature. 2007;446(7139):1023–9.
2. Collins BE, Paulson JC. Cell surface biology mediated by low affinity multivalent protein-glycan interactions. Curr Opin Chem Biol. 2004;8(6):617–25.
3. Zhao Y, Sato Y, Isaji T, Fukuda T, Matsumoto A, Miyoshi E, et al. Branched N-glycans regulate the biological functions of integrins and cadherins. FEBS J. 2008;275(9):1939–48.
4. Tang Z, Varghese RS, Bekesova S, Loffredo CA, Hamid MA, Kyselova Z, et al. Identification of N-glycan serum markers associated with hepatocellular carcinoma from mass spectrometry data. J Proteome Res. 2010;9(1):104–12.
5. Mechref Y, Madera M, Novotny MV. Glycoprotein enrichment through lectin affinity techniques. Methods Mol Biol. 2008;424: 373–96.
6. Mechref Y, Madera M, Novotny MV. Assigning glycosylation sites and microheterogeneities in glycoproteins by liquid chromatography/tandem mass spectrometry. In: Lipton MS, Paša-Tolic L, editors. Mass spectrometry of proteins and peptides: methods and protocols. Totowa: Humana Press; 2009. p. 161–80.
7. Leymarie N, Griffin PJ, Jonscher K, Kolarich D, Orlando R, McComb M, et al. Interlaboratory study on differential analysis of protein glycosylation by mass spectrometry: the ABRF glycoprotein research multi-institutional study 2012. Mol Cell Proteomics. 2013;12(10):2935–51.
8. Kolarich D, Jensen PH, Altmann F, Packer NH. Determination of site-specific glycan heterogeneity on glycoproteins. Nat Protoc. 2012;7(7):1285–98.
9. Petrescu AJ, Petrescu SM, Dwek RA, Wormald MR. A statistical analysis of N- and O-glycan linkage conformations from crystallographic data. Glycobiology. 1999;9(4):343–52.
10. Reinhold VN, Reinhold BB, Costello CE. Carbohydrate molecular weight profiling, sequence, linkage, and branching data: ES-MS and CID. Anal Chem. 1995;67(11):1772–84.
11. Laine RA. Information capacity of the carbohydrate code. Pure Appl Chem. 1997;69(9):1867–74.
12. Varki A. Sialic acids in human health and disease. Trends Mol Med. 2008;14(8):351–60.
13. Wuhrer M, Koeleman CA, Hokke CH, Deelder AM. Mass spectrometry of proton adducts of fucosylated N-glycans: fucose transfer between antennae gives rise to misleading fragments. Rapid Commun Mass Spectrom. 2006;20(11):1747–54.
14. Harvey DJ, Mattu TS, Wormald MR, Royle L, Dwek RA, Rudd PM. "Internal residue loss": rearrangements occurring during the fragmentation of carbohydrates derivatized at the reducing terminus. Anal Chem. 2002;74(4):734–40.

15. Reddy VA, Johnson RS, Biemann K, Williams RS, Ziegler FD, Trimble RB, et al. Characterization of the glycosylation sites in yeast external invertase. I. N-linked oligosaccharide content of the individual sequons. J Biol Chem. 1988;263:6978–85.

16. Li B, An HJ, Hedrick JL, Lebrilla CB. Collision-induced dissociation tandem mass spectrometry for structural elucidation of glycans. Methods Mol Biol. 2009;534:133–45.

17. Sleno L, Volmer DA. Ion activation methods for tandem mass spectrometry. J Mass Spectrom. 2004;39(10):1091–112.

18. Olsen JV, Macek B, Lange O, Makarov A, Horning S, Mann M. Higher-energy C-trap dissociation for peptide modification analysis. Nat Methods. 2007;4(9):709–12.

19. Takegawa Y, Deguchi K, Ito H, Keira T, Nakagawa H, Nishimura SI. Simple separation of isomeric sialylated N-glycopeptides by a zwitterionic type of hydrophilic interaction chromatography. J Sep Sci. 2006;29(16):2533–40.

20. Wuhrer M, de Boer AR, Deelder AM. Structural glycomics using hydrophilic interaction chromatography (Hilic) with mass spectrometry. Mass Spectrom Rev. 2009;28(2):192–206.

21. Alpert AJ, Shukla M, Shukla AK, Zieske LR, Yuen SW, Ferguson MAJ, et al. Hydrophilic-interaction chromatography of complex carbohydrates. J Chromatogr A. 1994;676(1):191–202.

22. Balaguer E, Demelbauer U, Pelzing M, Sanz-Nebot V, Barbosa J, Neususs C. Glycoform characterization of erythropoietin combining glycan and intact protein analysis by capillary electrophoresis–electrospray–time-of-flight mass spectrometry. Electrophoresis. 2006;27(13):2638–50.

23. Hermentin P, Doenges R, Witzel R, Hokke CH, Vliegenthart JF, Kamerling JP, et al. A strategy for the mapping of N-glycans by high-performance capillary electrophoresis. Anal Biochem. 1994;221(1):29–41.

24. Pu Y, Ridgeway ME, Glaskin RS, Park MA, Costello CE, Lin C. Separation and identification of isomeric glycans by selected accumulation-trapped ion mobility spectrometry-electron activated dissociation tandem mass spectrometry. Anal Chem. 2016;88(7):3440–3.

25. Michael C, Rizzi AM. Tandem mass spectrometry of isomeric aniline-labeled N-glycans separated on porous graphitic carbon: revealing the attachment position of terminal sialic acids and structures of neutral glycans. Rapid Commun Mass Spectrom. 2015;29(13):1268–78.

26. Dong X, Zhou S, Mechref Y. LC-MS/MS analysis of permethylated free oligosaccharides and N-glycans derived from human, bovine, and goat milk samples. Electrophoresis. 2016;37(11):1532–48.

27. Zhou S, Hu Y, Mechref Y. High-temperature LC-MS/MS of permethylated glycans derived from glycoproteins. Electrophoresis. 2016;37(11):1506–13.

28. Gray CJ, Thomas B, Upton R, Migas LG, Eyers CE, Barran PE, et al. Applications of ion mobility mass spectrometry for high throughput, high resolution glycan analysis. Biochim Biophys Acta. 2016;1860(8):1688–709.

29. Tousi F, Bones J, Hancock WS, Hincapie M. Differential chemical derivatization integrated with chromatographic separation for analysis of isomeric sialylated N-glycans: a nano-hydrophilic interaction liquid chromatography-MS platform. Anal Chem. 2013;85(17):8421–8.

30. Gimenez E, Sanz-Nebot V, Rizzi A. Relative quantitation of glycosylation variants by stable isotope labeling of enzymatically released N-glycans using [12C]/[13C] aniline and ZIC-HILIC-ESI-TOF-MS. Anal Bioanal Chem. 2013;405(23):7307–19.

31. Li H, Bendiak B, Siems WF, Gang DR, Hill Jr HH. Carbohydrate structure characterization by tandem ion mobility mass spectrometry (IMMS)2. Anal Chem. 2013;85(5):2760–9.

32. Yamaguchi Y, Nishima W, Re S, Sugita Y. Confident identification of isomeric N-glycan structures by combined ion mobility mass spectrometry and hydrophilic interaction liquid chromatography. Rapid Commun Mass Spectrom. 2012;26(24):2877–84.

33. Ruhaak LR, Lebrilla CB. Advances in analysis of human milk oligosaccharides. Adv Nutr. 2012;3(3):406s–14.

34. Creese AJ, Cooper HJ. Separation and identification of isomeric glycopeptides by high field asymmetric waveform ion mobility spectrometry. Anal Chem. 2012;84(5):2597–601.

35. Mechref Y. Analysis of glycans derived from glycoconjugates by capillary electrophoresis-mass spectrometry. Electrophoresis. 2011;32(24):3467–81.

36. Hua S, An HJ, Ozcan S, Ro GS, Soares S, DeVere-White R, et al. Comprehensive native glycan profiling with isomer separation and quantitation for the discovery of cancer biomarkers. Analyst. 2011;136(18):3663–71.

37. Brokl M, Hernandez-Hernandez O, Soria AC, Sanz ML. Evaluation of different operation modes of high performance liquid chromatography for the analysis of complex mixtures of neutral oligosaccharides. J Chromatogr A. 2011;1218(42):7697–703.

38. Yamagaki T, Sato A. Isomeric oligosaccharides analyses using negative-ion electrospray ionization ion mobility spectrometry combined with collision-induced dissociation MS/MS. Anal Sci. 2009;25(8):985–8.

39. Zhu M, Bendiak B, Clowers B, Hill Jr HH. Ion mobility-mass spectrometry analysis of isomeric carbohydrate precursor ions. Anal Bioanal Chem. 2009;394(7):1853–67.

40. Mechref Y, Novotny MV. Glycomic analysis by capillary electrophoresis-mass spectrometry. Mass Spectrom Rev. 2009;28(2):207–22.

41. Isailovic D, Kurulugama RT, Plasencia MD, Stokes ST, Kyselova Z, Goldman R, et al. Profiling of human serum glycans associated with liver cancer and cirrhosis by IMS-MS. J Proteome Res. 2008;7(3):1109–17.

42. Devakumar A, Mechref Y, Kang P, Novotny MV, Reilly JP. Identification of isomeric N-glycan structures by mass spectrometry with 157 nm laser-induced photofragmentation. J Am Soc Mass Spectrom. 2008;19(7):1027–40.

43. Atwood 3rd JA, Cheng L, Alvarez-Manilla G, Warren NL, York WS, Orlando R. Quantitation by isobaric labeling: applications to glycomics. J Proteome Res. 2008;7(1):367–74.

44. Broberg A. High-performance liquid chromatography/electrospray ionization ion-trap mass spectrometry for analysis of oligosaccharides derivatized by reductive amination and N,N-dimethylation. Carbohydr Res. 2007;342(11):1462–9.

45. Takegawa Y, Deguchi K, Keira T, Ito H, Nakagawa H, Nishimura S. Separation of isomeric 2-aminopyridine derivatized N-glycans and N-glycopeptides of human serum immunoglobulin G by using a zwitterionic type of hydrophilic-interaction chromatography. J Chromatogr A. 2006;1113(1–2):177–81.

46. Takegawa Y, Deguchi K, Ito S, Yoshioka S, Nakagawa H, Nishimura S. Simultaneous analysis of 2-aminopyridine-derivatized neutral and sialylated oligosaccharides from human serum in the negative-ion mode by sonic spray ionization ion trap mass spectrometry. Anal Chem. 2005;77(7):2097–106.

47. Gennaro LA, Harvey DJ, Vouros P. Reversed-phase ion-pairing liquid chromatography/ion trap mass spectrometry for the analysis of negatively charged, derivatized glycans. Rapid Commun Mass Spectrom. 2003;17(14):1528–34.

48. Que AH, Novotny MV. Structural characterization of neutral oligosaccharide mixtures through a combination of capillary electrochromatography and ion trap tandem mass spectrometry. Anal Bioanal Chem. 2003;375(5):599–608.

49. Anumula KR, Dhume ST. High resolution and high sensitivity methods for oligosaccharide mapping and characterization by normal phase high performance liquid chromatography following derivatization with highly fluorescent anthranilic acid. Glycobiology. 1998;8(7):685–94.

50. Karlsson H, Carlstedt I, Hansson GC. The use of gas chromatography and gas chromatography–mass spectrometry for the characterization of permethylated oligosaccharides with molecular mass up to 2300. Anal Biochem. 1989;182(2):438–46.

51. Bendiak B, Harris-Brandts M, Michnick SW, Carver JP, Cumming DA. Separation of the complex asparagine-linked oligosaccharides of the glycoprotein fetuin and elucidation of three triantennary structures having sialic acids linked only to galactose residues. Biochemistry. 1989;28(15):6491–9.

52. Royle L, Campbell MP, Radcliffe CM, White DM, Harvey DJ, Abrahams JL, et al. HPLC-based analysis of serum N-glycans on a 96-well plate platform with dedicated database software. Anal Biochem. 2008;376(1):1–12.

53. Campbell MP, Royle L, Radcliffe CM, Dwek RA, Rudd PM. GlycoBase and autoGU: tools for HPLC-based glycan analysis. Bioinformatics. 2008;24(9):1214–6.

54. Nwosu C, Yau HK, Becht S. Assignment of core versus antenna fucosylation types in protein N-glycosylation via procainamide labeling and tandem mass spectrometry. Anal Chem. 2015;87(12):5905–13.

55. Wuhrer M. Glycomics using mass spectrometry. Glycoconj J. 2013;30(1):11–22.

56. Hakomori S. A rapid permethylation of glycolipid, and polysaccharide catalyzed by methylsulfinyl carbanion in dimethyl sulfoxide. J Biochem. 1964;55:205–8.

57. Kang P, Mechref Y, Klouckova I, Novotny MV. Solid-phase permethylation of glycans for mass spectrometric analysis. Rapid Commun Mass Spectrom. 2005;19(23):3421–8.

58. Viseux N, de Hoffmann E, Domon B. Structural analysis of permethylated oligosaccharides by electrospray tandem mass spectrometry. Anal Chem. 1997;69(16):3193–8.

59. Viseux N, de Hoffmann E, Domon B. Structural assignment of permethylated oligosaccharide subunits using sequential tandem mass spectrometry. Anal Chem. 1998;70(23):4951–9.

60. Weiskopf AS, Vouros P, Harvey DJ. Characterization of oligosaccharide composition and structure by quadrupole ion trap mass spectrometry. Rapid Commun Mass Spectrom. 1997;11(14):1493–504.

61. Weiskopf AS, Vouros P, Harvey DJ. Electrospray ionization-ion trap mass spectrometry for structural analysis of complex N-linked glycoprotein oligosaccharides. Anal Chem. 1998;70(20):4441–7.

62. Sheeley DM, Reinhold VN. Structural characterization of carbohydrate sequence, linkage, and branching in a quadrupole Ion trap mass spectrometer: neutral oligosaccharides and N-linked glycans. Anal Chem. 1998;70(14):3053–9.

63. Ciucanu I, Costello CE. Elimination of oxidative degradation during the per-O-methylation of carbohydrates. J Am Chem Soc. 2003;125(52):16213–9.

64. Linsley KB, Chan SY, Chan S, Reinhold BB, Lisi PJ, Reinhold VN. Applications of electrospray mass spectrometry to erythropoietin N- and O-linked glycans. Anal Biochem. 1994;219(2):207–17.

65. Costello CE, Contado-Miller JM, Cipollo JF. A glycomics platform for the analysis of permethylated oligosaccharide alditols. J Am Soc Mass Spectrom. 2007;18(10):1799–812.

66. Abrahams JL, Packer NH, Campbell MP. Relative quantitation of multi-antennary N-glycan classes: combining PGC-LC-ESI-MS with exoglycosidase digestion. Analyst. 2015;140(16):5444–9.

67. Everest-Dass AV, Abrahams JL, Kolarich D, Packer NH, Campbell MP. Structural feature ions for distinguishing N- and O-linked glycan isomers by LC-ESI-IT MS/MS. J Am Soc Mass Spectrom. 2013;24(6):895–906.

68. Everest-Dass AV, Jin D, Thaysen-Andersen M, Nevalainen H, Kolarich D, Packer NH. Comparative structural analysis of the glycosylation of salivary and buccal cell proteins: innate

69. protection against infection by *Candida albicans*. Glycobiology. 2012;22(11):1465–79.

69. Everest-Dass AV, Kolarich D, Campbell MP, Packer NH. Tandem mass spectra of glycan substructures enable the multistage mass spectrometric identification of determinants on oligosaccharides. Rapid Commun Mass Spectrom. 2013;27(9):931–9.

70. Lee A, Nakano M, Hincapie M, Kolarich D, Baker MS, Hancock WS, et al. The lectin riddle: glycoproteins fractionated from complex mixtures have similar glycomic profiles. OMICS. 2010;14(4):487–99.

71. Sumer-Bayraktar Z, Kolarich D, Campbell MP, Ali S, Packer NH, Thaysen-Andersen M. N-glycans modulate the function of human corticosteroid-binding globulin. Mol Cell Proteomics. 2011;10(8): M111 009100.

72. Hu Y, Shihab T, Zhou S, Wooding K, Mechref Y. LC–MS/MS of permethylated N-glycans derived from model and human blood serum glycoproteins. Electrophoresis. 2016;37(11):1498–505.

73. Tarentino AL, Plummer Jr TH. Enzymatic deglycosylation of asparagine-linked glycans: purification, properties, and specificity of oligosaccharide-cleaving enzymes from *Flavobacterium meningosepticum*. Methods Enzymol. 1994;230:44–57.

74. Huang Y, Konse T, Mechref Y, Novotny MV. Matrix-assisted laser desorption/ionization mass spectrometry compatible beta-elimination of O-linked oligosaccharides. Rapid Commun Mass Spectrom. 2002;16(12):1199–204.

75. Segu ZM, Mechref Y. Characterizing protein glycosylation sites through higher-energy C-trap dissociation. Rapid Commun Mass Spectrom. 2010;24(9):1217–25.

76. Hu Y, Mayampurath A, Khan S, Cohen JK, Mechref Y, Volchenboum SL. N-linked glycan profiling in neuroblastoma cell lines. J Proteome Res. 2015;14(5):2074–81.

77. Zacharias LG, Hartmann AK, Song E, Zhao J, Zhu R, Mirzaei P, et al. HILIC and ERLIC enrichment of glycopeptides derived from breast and brain cancer cells. J Proteome Res. 2016;12:12.

78. Hu Y, Zhou S, Khalil SI, Renteria CL, Mechref Y. Glycomic profiling of tissue sections by LC-MS. Anal Chem. 2013;85(8): 4074–9.

79. Reinhold V, Zhang H, Hanneman A, Ashline D. Toward a platform for comprehensive glycan sequencing. Mol Cell Proteomics. 2013;12(4):866–73.

80. Ueda K. Glycoproteomic strategies: from discovery to clinical application of cancer carbohydrate biomarkers. Proteomics Clin Appl. 2013;7(9–10):607–17.

81. Zaia J. Capillary electrophoresis-mass spectrometry of carbohydrates. Methods Mol Biol. 2013;984:13–25.

82. Zhang Y, Yin H, Lu H. Recent progress in quantitative glycoproteomics. Glycoconj J. 2012;29(5–6):249–58.

83. Gupta G, Surolia A, Sampathkumar SG. Lectin microarrays for glycomic analysis. OMICS. 2010;14(4):419–36.

84. Zaia J. Mass spectrometry and the emerging field of glycomics. Chem Biol. 2008;15(9):881–92.

85. Larsen K, Thygesen MB, Guillaumie F, Willats WG, Jensen KJ. Solid-phase chemical tools for glycobiology. Carbohydr Res. 2006;341(10):1209–34.

86. Hirabayashi J. Lectin-based structural glycomics: glycoproteomics and glycan profiling. Glycoconj J. 2004;21(1–2):35–40.

87. Feizi T, Fazio F, Chai W, Wong CH. Carbohydrate microarrays—a new set of technologies at the frontiers of glycomics. Curr Opin Struct Biol. 2003;13(5):637–45.

88. Chandler KB, Costello CE. Glycomics and glycoproteomics of membrane proteins and cell-surface receptors: present trends and future opportunities. Electrophoresis. 2016;37(11):1407–19.

89. Mereiter S, Balmana M, Gomes J, Magalhaes A, Reis CA. Glycomic approaches for the discovery of targets in gastrointestinal cancer. Front Oncol. 2016;6:55.

90. Yang S, Rubin A, Eshghi ST, Zhang H. Chemoenzymatic method for glycomics: isolation, identification, and quantitation. Proteomics. 2016;16(2):241–56.

91. Stavenhagen K, Kolarich D, Wuhrer M. Clinical glycomics employing graphitized carbon liquid chromatography-mass spectrometry. Chromatographia. 2015;78(5–6):307–20.

92. Mechref Y, Hu Y, Desantos-Garcia JL, Hussein A, Tang H. Quantitative glycomics strategies. Mol Cell Proteomics. 2013;12(4):874–84.

93. Song E, Mechref Y. Defining glycoprotein cancer biomarkers by MS in conjunction with glycoprotein enrichment. Biomark Med. 2015;9(9):835–44.

94. Novotny MV, Mechref Y. New hyphenated methodologies in high-sensitivity glycoprotein analysis. J Sep Sci. 2005;28(15):1956–68.

95. Orlando R. Quantitative analysis of glycoprotein glycans. Methods Mol Biol. 2013;951:197–215.

96. Orlando R. Quantitative glycomics. Methods Mol Biol. 2010;600:31–49.

97. Tharmalingam T, Adamczyk B, Doherty MA, Royle L, Rudd PM. Strategies for the profiling, characterisation and detailed structural analysis of N-linked oligosaccharides. Glycoconj J. 2013;30(2):137–46.

98. Marino K, Bones J, Kattla JJ, Rudd PM. A systematic approach to protein glycosylation analysis: a path through the maze. Nat Chem Biol. 2010;6(10):713–23.

99. Tretter V, Altmann F, Marz L. Peptide-N4-(N-acetyl-beta-glucosaminyl)asparagine amidase F cannot release glycans with fucose attached alpha 1−3 to the asparagine-linked N-acetylglucosamine residue. Eur J Biochem. 1991;199(3):647–52.

100. Berman E, Bendel P. One- and two-dimensional 90.5-MHz ^{13}C-NMR spectroscopy of the N-linked triantennary oligosaccharide units of calf fetuin. FEBS Lett. 1986;204(2):257–60.

101. Cumming DA, Hellerqvist CG, Harris-Brandts M, Michnick SW, Carver JP, Bendiak B. Structures of asparagine-linked oligosaccharides of the glycoprotein fetuin having sialic acid linked to N-acetylglucosamine. Biochemistry. 1989;28(15):6500–12.

102. Green ED, Adelt G, Baenziger JU, Wilson S, Van Halbeek H. The asparagine-linked oligosaccharides on bovine fetuin. Structural analysis of N-glycanase-released oligosaccharides by 500-megahertz ^{1}H NMR spectroscopy. J Biol Chem. 1988;263(34):18253–68.

103. Wong-Madden ST, Landry D. Purification and characterization of novel glycosidases from the bacterial genus Xanthomonas. Glycobiology. 1995;5(1):19–28.

104. Taron CH, Benner JS, Hornstra LJ, Guthrie EP. A novel beta-galactosidase gene isolated from the bacterium Xanthomonas manihotis exhibits strong homology to several eukaryotic beta-galactosidases. Glycobiology. 1995;5(6):603–10.

105. Zhou S, Hu Y, Veillon L, Snovida SI, Rogers JC, Saba J, et al. Quantitative LC–MS/MS glycomic analysis of biological samples using aminoxyTMT. Anal Chem. 2016;88(15):7515–22.